

Preliminary SANS studies of the structure of nickel powders on the nanoscale

R.B. Knott^{a,*}, M. Lin^b, H.J.M. Hanley^c, D. Muir^d

^a*Australian Nuclear Science and Technology Organisation, Private Mail Bag, Menai 2234 NSW, Australia*

^b*National Institute of Standards and Technology, 100 Bureau Drive, Gaithersburg 20899 MD, USA*

^c*National Institute of Standards and Technology, Boulder 80305 CO, USA*

^d*WMC Resources Australia Pty Ltd, Perth 6000 WA, Australia*

Abstract

Nickel powders produced by hydrogen reduction of nickel ammine/ammonium sulphate solution were examined for their structure on the nanoscale using the small-angle neutron scattering (SANS) technique. It is known that the particle size and density of the powder depends on the number of times the nickel solution bath was subjected to hydrogen reduction, however the porosity on the nanoscale is open to question. Porosity in commercial nickel powders is a concern since these nanopores can trap sulphur impurities from solution and lead to unacceptably high levels of sulphur in the final nickel product. SANS data over the q -range (0.002 – 0.18 \AA^{-1}) was collected on nickel powders that had been exposed to 0, 1, 2, 40, and 60 cycles of hydrogenation in an industrial refining process. Results from this study indicate general trends in the nanostructure consistent with a roughening of the surface with the power law exponent in the Porod region consistently exceeding 4. Further experiments are required to clarify the overall porosity. Crown Copyright © 2006 Published by Elsevier B.V. All rights reserved.

PACS: 61.12.Ex; 61.43.Gt

Keywords: Nickel powder; SANS; Porosity; Fractal properties

1. Introduction

Nickel (Ni) is a lustrous white, hard, ferromagnetic metal found in transition group VIII of the Periodic Table. It has high ductility, good thermal conductivity, high strength, and fair electrical conductivity. Nickel is an important metal commercially because of its marked resistance to corrosion and oxidation in both air and aqueous environments. It is of primary importance in the manufacture of steel alloys, and has had a major role in the development of the chemical and aerospace industries. It constitutes approximately 0.008% of the earth's crust, making it the 24th most abundant element. Nickel can achieve several oxidation states including -1 , 0 , $+1$, $+2$, $+3$, and $+4$; however, the majority of nickel compounds are nickel $+2$ species. Nickel does not occur in nature as pure metal but

as a component of other minerals. The most prevalent forms of nickel minerals are sulphides, oxides, silicates, and arsenates, and all but the arsenates are important nickel minerals from a mining and natural resource perspective.

Nickel is produced from two very different ores, lateritic and sulphidic. Lateritic ores are normally found in tropical climates where weathering, with time, extracts and deposits the ore in layers at varying depths below the surface. Sulphidic ores, often found in conjunction with copper-bearing ores, are usually mined from underground. The most common nickel sulphide mineral, pentlandite $[(\text{NiFe})_9\text{S}_8]$, presently accounts for the majority of the nickel produced in the world.

The main ore nickel in Australia (and in terms of worldwide production) is pentlandite, which occurs with pyrrhotite ($\text{Fe}_n\text{S}_{n+1}$), pyrite (FeS), and chalcopyrite (CuFeS_2) in lodes in mafic and ultramafic (iron and magnesium-rich) igneous rocks. In Australia, nickeliferous sulphide ores and their host rocks mainly form parts of

*Corresponding author. Tel.: +61 2 9717 3218; fax: +61 2 9717 3606.

E-mail address: rbk@ansto.gov.au (R.B. Knott).

ancient volcanic lavaflores. However, most of the world's known reserves are contained in nickel-bearing laterites (such as in New Caledonia and Cuba) in minerals such as garnierite ($(\text{NiMg})\text{SiO}_3 \cdot n\text{H}_2\text{O}$) and nickeliferous limonite (nickel mixed with hydrated iron oxide). The nickel grade of sulphide ore typically ranges from 1–4%, and that of lateritic ore from 1–2%.

After mining, the sulphide ores are concentrated to increase their nickel content. The ores are first crushed and ground, liberating the sulphide minerals from worthless rock or gangue. The sulphide minerals are then separated from the gangue by flotation and dried. The material is then typically sent to a smelter, which uses an Outokumpu flash furnace or similar to produce nickel matte (essentially a mixture of nickel and iron sulphides), containing ~71–72% Ni and ~5–6% Cu. The nickel matte is produced in granulated form and used for feed in a nickel refinery.

The refining process uses a hydrometallurgical ammonia leach process, which involves leaching the nickel matte with ammonia at 85 °C and high pressure. This dissolves the nickel as an ammonia complex while precipitating many metal impurities in the feed slurry. After oxydrolisis, which removes the ammonia, hydrogen is passed through the solution at high pressure and temperatures to produce a nickel powder. The remaining solution is rich in ammonium sulphate, which is crystallized as an agricultural fertilizer. The nickel is dried to a powder, or compacted and heated to form sintered briquettes. At this stage it is ~99% pure.

The purity of the final nickel metal product is dependent on the porosity, since porous briquettes can entrap sulphur impurities (present in the refining solution) and degrade the final product significantly.

The small angle neutron scattering (SANS) technique provides valuable information of the structure on the nanoscale of a wide variety of systems from biological molecules in solution, to hard-condensed matter. Neutrons are a non-destructive probe of bulk materials and are well suited to investigating the structure of complex industrial materials. In this case, evidence was sought for the origin and nature of the porosity and surface structure of nickel powders produced by an industrial refining process.

2. Method

Five powder samples—corresponding to 0, 1, 2, 40 and 60 recycles—were obtained from the industrial refinery. An equal weight of each sample was placed in a quartz-window cell, with pathlength 1 mm, and the cells placed in the neutron beam. Two SANS instruments at the NIST Center for Neutron Research (NCNR Gaithersburg USA) [1] were used for these studies. The 8 m SANS instrument was configured with 3.6 m sample–detector distance and an incident neutron wavelength, λ , of 6 Å (25% $\Delta\lambda/\lambda$). The 30 m SANS was configured with 15 m sample to detector distance and an incident neutron wavelength of 6 Å (22%

$\Delta\lambda/\lambda$). The combined scattering vector range was $0.002 < q < 0.18 \text{ \AA}^{-1}$ (where $q = (4\pi/\lambda) \sin(\theta)$ and 2θ is the scattering angle).

The scattering intensity, $I(q)$, was corrected for electronic background, sample transmission and thickness, empty-cell scattering, and detector inhomogeneity; and placed on an absolute scale using a secondary standard (porous silica). The 2D patterns were radially averaged to produce 1D SANS profiles. As will be shown later, Porod scattering dominated the experimental data, therefore, a power law was fitted to the 1D SANS profiles

$$I(q) = Aq^p + B, \quad (2.1)$$

where A is a constant proportional to the neutron contrast, p is the power law exponent, and B the background term. The data were reduced and analysed using IGOR software (Wavemetrics Inc., USA).

3. Results and discussion

Fig. 1 is a plot of the scattered intensity $I(q)$ per unit mass (in units of $\text{cm}^{-1}/\text{density}$) versus q (\AA^{-1}) from the powders as a function of the number of hydrogen cycles.

Full analysis of the data will be carried out after more experimentation and will follow the procedures discussed in the literature [2,3]. The preliminary evaluation, however, is that the experiment is consistent with a growth, or increase in a characteristic dimension, of the nickel powder as the hydrogen reduction proceeds. For example:

1. All intensity profiles decrease with q with a power law exponent of 3.7–4.0 over a wide range. It is, therefore, suggested that surface Porod scattering dominates.
2. The relative intensity decreases with increased hydrogenation, indicating a decline in surface area.
3. The early cycles suggest—since the curves tend to flatten at lower q —a characteristic length (a particle or pore size or pore distribution) of ~800 Å. This length goes to low- q , and thus increases, as the hydrogen cycles increase; a result consistent with electron and optical microscopy [4].

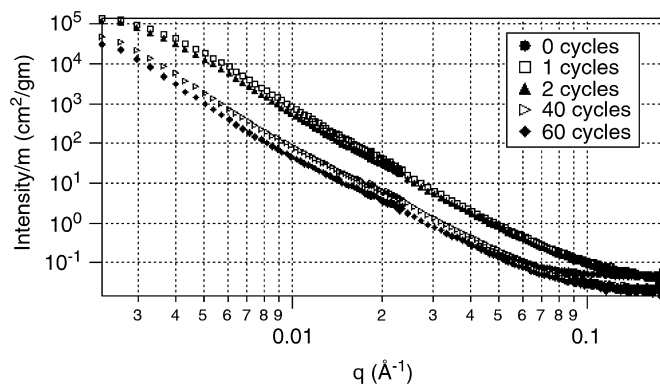


Fig. 1. 1D SANS profiles of nickel powder extracted from an industrial-scale nickel refining process. Note that error bars are small and have been omitted for clarity.

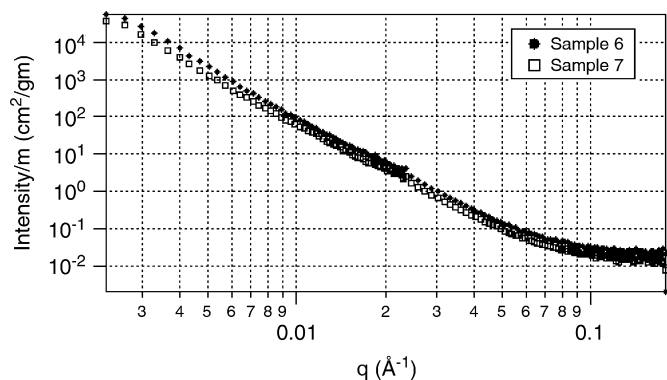


Fig. 2. 1D SANS profiles of two hydrogenated samples. Note that error bars are small and have been omitted for clarity.

Table 1
Results of power law fit to 1D SANS profiles for nickel samples extracted from an industrial refining process

Sample	# Cycles	P	A	B
1	0	−3.75	1.56	0.018
2	1	−4.13	2.36	0.062
3	2	−3.98	4.83	0.044
4	40	−3.80	2.21	0.023
5	60	−3.75	1.52	0.047
6		−4.19	0.49	0.023
7		−4.17	0.35	0.016

4. Increased high- q scattering from the late-cycle runs may well indicate the onset of another, shorter, length indicating the appearance of void spaces.

Two nickel powder samples were provided that were heated to 800 °C for 30 min in a hydrogen–nitrogen gas mixture; the objective being to remove any sulphur as H₂S. Fig. 2 shows the 1D SANS profiles.

Note that the upturn in $I(q)$ at high- q is present, as expected. Of more interest, however, is that the power law exponent is ~ 4.2 , greater than the Porod value of 4.0. Exactly why the exponent is >4 is an open and interesting question [5–8] but is most probably the consequence of a scattering length gradient at the surface caused, for example, by surface degradation, a variation from fractal roughness, or a variation in chemical composition.

The results of fitting a power law to the data are summarized in Table 1. The fitting q -range was typically $0.007 < q < 0.15 \text{ \AA}^{-1}$ and the error on p typically ± 0.01 .

The entire data collection procedure was repeated for samples 4 and 5, and the results are within experimental error. This is an important result given the origin of the samples (i.e. a complex industrial process) and the potential difficulty of SANS from fine, powdered samples.

4. Conclusion

In summary, it is suggested that the high-temperature hydrogenation did not change the morphology of the nickel powder significantly but rather reacted in some way with the particle surface.

Future experiments will focus on the industrial objectives, and will include more extensive SANS intensity measurements at low- and high- q , especially for samples made from early hydrogen reduction cycles. The SANS experiments and data analysis will be formulated to distinguish between particle size, pore size and void space. Finally, the SANS data must be coordinated with electron and optical microscopy, and with experiments that give an insight into the chemical contaminants of the powder.

Acknowledgements

The authors gratefully acknowledge the support of the National Institute of Standards and Technology, US Department of Commerce, in providing the neutron research facilities used in this work. This work utilized facilities supported in part by the National Science Foundation under Agreement no. DMR-9986442.

References

- [1] B. Hammouda, S. Krueger, C.J. Glinka, J. Res. Nat. Instrum. Stand. Technol. 98 (1993) 31.
- [2] P. McMahan, I. Snook, J. Chem. Phys. 105 (1996) 1.
- [3] A.J. Allen, J. Appl. Crystallogr. 24 (1991) 624.
- [4] Optical data provided by WMC Technology.
- [5] P.W. Schmidt, D. Avnir, D. Levy, A. Hoehr, M. Steiner, A. Roell, J. Chem. Phys. 94 (1991) 1474.
- [6] P.J. McMahan, I. Snook, E. Smith, J. Chem. Phys. 114 (2001) 8223.
- [7] A.J. Hurd, D. Schaefer, D.M. Smith, S.B. Ross, A. Le Méhauté, S. Spooner, Phys. Rev. B 39 (1989) 9742.
- [8] H.D. Bale, P.W. Schmidt, Phys. Rev. Lett. 53 (1984) 596.